of **1**, **9**, and **2** in the ratio ca. 1:2:1 in the equilibrium mixture from **2a**, implies that this equilibrium condition is fulfilled.
(31) In order to obtain a reasonable value of *R* the reaction should not have been allowed to proceed too far toward equilibrium. In order to obtain maximum accuracy in the assessment of peak areas, especially in the case of Figure 3 described below, it was necessary to proceed well toward equilibrium. A compromise is therefore necessary.
(32) Similar small differences in rate coefficient were observed in the reaction between neutral cobalt(II) species and alkyl halides.[33]
(33) P. W. Schneider, P. F. Phelan, and J. Halpern, *J. Am. Chem. Soc.*, **91**, 77 (1969).
(34) M-N. Richroch, C. Bied-Charreton, and A. Gaudemer, *Tetrahedron Lett.*, 2859 (1971); M-N. Richroch, Thesis, Universite de Paris-Sud, Centre d'Orsay, 1975, CNRS No. A 9934.
(35) K. N-V. Duong, A. Ahond, C. Merrienne, and A. Gaudemer, *J. Organomet. Chem.*, **55**, 375 (1973).
(36) Reference 1, p 224.
(37) Since the submission of this manuscript we have discovered a host of reactions involving concerted homolytic displacement of cobaloxime(II) by organic free radicals, e.g., T. Funabiki, B. D. Gupta, and M. D. Johnson, *J. Am. Chem. Soc.*, **98**, 6697 (1976).
(38) M. Julia, *Pure Appl. Chem.*, **40**, 553 (1974).
(39) E. A. Stadlbauer, R. J. Holland, F. P. Lamm, and G. N. Schrauzer, *Bioinorg. Chem.*, **4**, 67 (1974).
(40) G. Agnes, H. A. O. Hill, J. M. Pratt, S. C. Ridsdale, F. S. Kennedy, and R. J. P. Williams, *Biochim. Biophys. Acta*, **252**, 207 (1971).
(41) C. Bied-Charreton, C. J. Cooksey, A. Gaudemer, and M. D. Johnson, unpublished observations.
(42) It is pertinent to assume that reaction 15 involves inversion, though the alternative retention process should be considered as well.
(43) In all three transition states of *this kind*, the two cobalt atoms will be identical, though in principle a pair of identical transition states may be concerned on either side of a symmetrical intermediate.
(44) $E_{1/2}$ for cobaloxime(II) → cobaloxime(I) in pyridine at 0 °C is -1.24 V (vs. SCE). G. Costa, G. Mestroni, A. Puxeddu, and E. Reisenhofer, *J. Chem. Soc. A*, 2870 (1970).
(45) $E_{1/2}$ for alkyl(aquo)cobaloxime(III) → alkyl(aquo)cobaloxime(IV) in water, ca. 0.9 V. J. Halpern, M. S. Chan, J. Hanson, T. S. Roche, and J. A. Topich, *J. Am. Chem. Soc.*, **97**, 1606 (1975).
(46) J. Devinq, unpublished observations.
(47) G. N. Schrauzer, *Inorg. Synth.* **11**, 61 (1968); S. N. Anderson, D. H. Ballard, and M. D. Johnson, *J. Chem. Soc., Perkin Trans. 2*, 311 (1972).

The Carbonyl Scrambling Processes in the Isomeric Pentacarbonylguaiazulenediiron and Homologous Ruthenium Molecules; a Novel Mechanism for the Internuclear Processes

F. Albert Cotton,* Brian E. Hanson, John R. Kolb, Pascual Lahuerta,[1] George G. Stanley, B. Ray Stults, and Alan J. White

Contribution from the Department of Chemistry, Texas A&M University, College Station, Texas 77843. *Received October 12, 1976*

Abstract: The structural and dynamic properties of five compounds of the type $XM_2(CO)_4L$, namely, the geometric isomers **1**, **2** (X = guaiazulene, M = Fe, L = CO), the geometric isomers **3**, **4** (X = guaiazulene, M = Ru, L = CO), and **5** (X = guaiazulene, M = Fe, L = PEt_3), have been studied. In all cases the CO scrambling processes have been studied over a wide temperature range using ^{13}C NMR. For compounds **1**, **2**, and **5** the molecular and crystal structures have been determined by x-ray crystallography. **1** forms triclinic crystals: $P\bar{1}$, $a = 13.627$ (7) Å, $b = 16.993$ (8) Å, $c = 8.782$ (3) Å, $\alpha = 98.78$ (3)°, $\beta = 99.79$ (3)°, $\gamma = 95.34$ (4)°, $V = 1965.6$ (15) Å^3, $Z = 4$. The structure was refined with Fe atoms only anisotropic to $R_1 = 0.12$ and $R_2 = 0.11$. The two molecules in the asymmetric unit are essentially identical and have the $Fe(CO)_3$ group bound to an allylic moiety that does not bear the isopropyl substituent. The mean Fe–Fe distance is 2.791 (10) Å. **2** also forms triclinic crystals: $P\bar{1}$, $a = 12.286$ (4) Å, $b = 14.297$ (3) Å, $c = 11.029$ (3) Å, $\alpha = 90.22$ (2)°, $\beta = 95.72$ (2)°, $\gamma = 97.54$ (2)°, $V = 1910.9$ (8) Å^3, $Z = 4$. This structure was refined with only the iron atoms anisotropic to $R_1 = 0.068$ and $R_2 = 0.085$. The two molecules in the asymmetric unit are chemically identical with the $Fe(CO)_3$ group bound to an allylic moiety having the isopropyl group attached to the center carbon atom. The mean Fe–Fe bond length is 2.808 (4) Å. **5** forms monoclinic crystals: $P2_1/n$, $a = 12.487$ (5) Å, $b = 13.918$ (5) Å, $c = 15.196$ (6) Å, $\beta = 103.90$ (3)°, $V = 2563.6$ (16) Å^3, $Z = 4$. The structure was refined to $R_1 = 0.075$ and $R_2 = 0.085$ with anisotropic temperature factors assigned to the iron atoms, carbonyl C and O atoms, and the P atom only. The structure is derived from that of **1** by replacing the CO group trans to the Fe–Fe bond by PEt_3. The Fe–Fe bond length is 2.800 (4) Å.

For several years we have been studying carbonyl scrambling processes in the class of binuclear molecules that have an $(OC)_nM{-}M'(CO)_m$ moiety bonded to a cyclic, or bicyclic, polyene or polyenyl group. This general formulation includes the common symmetrical case where $M = M'$ and $n = m$, as well as more general cases. Those that we have studied included **6–13**. In this paper we present a detailed report of the structural and dynamic properties of compounds **1–5**. The background for the present work is provided by our previous studies of compounds **6–13**, and we shall therefore begin by summarizing the salient features of compounds **6–13**.

In compound **6**, it was found[2] that the signals for the tricarbonyl moiety coalesce at about 0 °C, whereas up to at least 75 °C, the signal for the equivalent CO groups in the $Fe(CO)_2$ moiety remains distinct and sharp. Thus, no evidence for internuclear scrambling is seen up to 75 °C.

In **7** coalescence that we believe to be (but cannot prove to be) due only to local scrambling within each of the equivalent $Fe(CO)_3$ groups occurs[2] at about -14 °C.

In the related compounds **8**, **9**, and **10**, *only localized* scrambling processes occur,[3,4] with coalescence temperatures ranging from ca. -80 to ca. $+60$ °C.

In compound **11**[5,6] and the related (guaiazulene)$W_2(CO)_6$[7] and (azulene)$Mo_2(CO)_6$[7] only localized scrambling occurs.

In our most recent paper[8] in this area on **12** and **13**, we have shown that carbonyl scrambling occurs in two well-defined stages. First, localized scrambling in the $M(CO)_3$ group becomes rapid enough to give a single line (T_c = ca. -70 °C for Fe, ca. -15 °C for Ru), after which there is general (i.e., internuclear) scrambling. These systems, (azulene)$M_2(CO)_5$, were the first ones in the general group under consideration here in which internuclear scrambling was observed. In re-

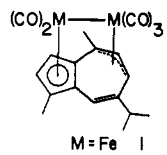

M = Fe 1
Ru 3

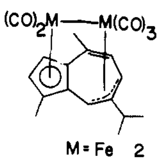

M = Fe 2
Ru 4

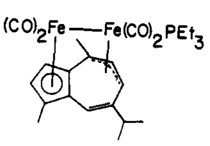

5

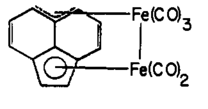

6

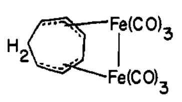

7

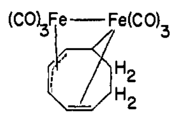

B

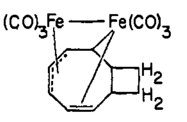

9

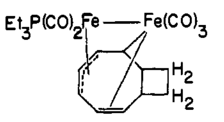

10

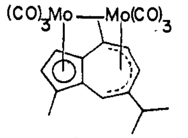

11

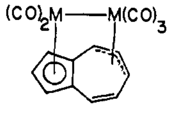

M = Fe 12
Ru 13

porting these observations it was explicitly noted that (a) no choice could be made between several possible pathways, and (b) there was no evident reason why internuclear scrambling is observed in **12** but not in **6** or, for that matter, in **8**, **9**, and **10**. Obviously, if we could answer the first of these two questions we might be better able to answer the second.

In the present paper we report out studies of compounds **1–5**, which were undertaken with the purpose of getting information that might help us to answer either or both questions. We believe that the data now in hand do allow us to suggest reasonable answers to both questions.

Experimental Section

General Procedures. All operations involving air-sensitive materials were carried out in an atmosphere of nitrogen or argon using standard techniques.[9] Photochemical reactions were carried out in Pyrex vessels using a Norelco 250-W high-pressure mercury lamp. Infrared spectra of hexane solutions were recorded on a Perkin-Elmer Model 467 spectrophotometer. Proton NMR spectra were recorded in $CDCl_3$ on an HA-100D spectrometer locked on Me_4Si or benzene. Melting points were recorded under argon on a Thomas-Kofler melting point apparatus equipped with inert atmosphere attachment. Carbon-13 NMR spectra were recorded on a JEOL PFT 100/Nicolet 1080 Fourier transform spectrometer operating at 25.036 MHz. A sweep width of 7000 Hz and a repetition rate of 1.1 s were employed. The temperatures, measured with a copper-constantan thermocouple inserted into an NMR tube and read on a Leads and Northrup Model 913 digital thermometer, were constant to within ±1°. For the $(C_{15}H_{18})Fe_2(CO)_5$ isomers the spectra were recorded from −100 to +60 °C in acetone-d_6 (95%) which served as an internal lock signal and CS_2 (5%) as a reference standard. Below −100 °C the solvent system employed was 80% 2-methyltetrahydrofuran, 15% acetone-d_6, and 5% CS_2. Above 60 °C the solvent system was 95% C_6D_6 and 5% CS_2. For the iron system the number of transients necessary to yield acceptable spectra varied from 2000 scans at the lowest temperatures to 3600 scans at 80 °C.

The carbon-13 NMR spectra for $(C_{15}H_{18})Ru_2(CO)_5$ isomer 1 were recorded in CD_2Cl_2 (25%), 2-methyltetrahydrofuran (70%), and Me_4Si (5%). The spectra for isomer 2 were recorded in CD_2Cl_2 (45%), CCl_3CH_3 (50%), and Me_4Si (5%) from −99 to 25 °C. Spectra above 25 °C were recorded in C_6D_6 (20%), toluene (75%), and Me_4Si (5%). Chemical shifts were measured from Me_4Si. The instrument was locked on deuterium collecting 5000 transients at −99 °C to 9000 transients at 122 °C.

Preparation of Compounds. (Guaiazulene)$Fe_2(CO)_5$. Guaiazulenediiron pentacarbonyl was prepared by the thermal reaction of guaiazulene with a large excess of iron pentacarbonyl.[10] In contrast to the earlier report, we find that the reaction, when carried out in refluxing isooctane, is essentially complete within 1 day and further refluxing leads only to decomposition of excess $Fe(CO)_5$. After filtration and removal of solvent and remaining $Fe(CO)_5$ under vacuum, separation and purification of the two isomers were accomplished by chromatography using 1/4 $CHCl_3$-petroleum ether (bp 30-60 °C) as eluent. As was reported by Burton et al.,[10] we find the two isomers to be present in approximately equal amounts when synthesized in the manner described. It was necessary to separate the isomers on a 120 × 2.5 cm column of Woelm activity grade II neutral alumina. Crystallization of each isomer was effected in *n*-pentane. The isomers, which we shall designate 1 and 2, in the order of elution, were shown to be identical with those reported by Burton et al.,[10] by their infrared spectra, ^1H NMR spectra, and melting point.

A 5-g sample of guaiazulenediiron pentacarbonyl (ca. 1:1 mixture of isomers) was enriched in ^{13}CO by dissolving it in 200 mL of hexane in a 500-mL single-necked Pyrex flask equipped with a side arm and magnetic stirbar. The solution was freeze-thaw degassed and refrozen and the space above evacuated. The flask was then refilled to a pressure of 1 atm with CO enriched to 90% in ^{13}C, sealed, and irradiated for 20 h. The solvent was removed and the resulting oil was crystallized from pentane at −78 °C. The enriched sample was reserved for the reaction described below. The level of enrichment (ca. 10%) was monitored by infrared spectrophotometry.

Reactions of (Guaiazulene)$Fe_2(CO)_5$ with PEt_3. Two reactions were performed. In the first, 0.8 g (1.8 mmol) of (guaiazulene)$Fe_2(CO)_5$, isomer 1, 0.4 mL (4.1 mmol) of PEt_3, and 50 mL of benzene were irradiated for 20 h in a Pyrex flask fitted with a reflux condenser and gas adaptor. The solvent was removed under vacuum leaving a brown oil which was taken up in 1:4 benzene-hexane and chromatographed. Guaiazulene and unreacted starting material were eluted with 1:4 benzene-hexane. A dark red band was eluted by increasing the proportion of benzene to 1:1. Solvent was removed to give a dark red oil which was crystallized from pentane at −12 °C. The red solid has a melting point of 93-94 °C and shows only two strong absorptions in the ν_{CO} region, at 1990 and at 1938 cm^{-1}. Several other variously colored bands could be eluted from the column with diethyl ether but were not investigated further.

In the second reaction 3.2 g (7.1 mmol) of guaiazulenediiron pentacarbonyl (ca. 1:1 isomeric mixture, 10% enriched in ^{13}CO) and 1.6 mL (16.7 mmol) of PEt_3 were dissolved in 15 mL of benzene and irradiated for 41 h. The reaction mixture was evaporated to give a brown oil which was chromatographed. Elution with 1:4 benzene-hexane brought down guaiazulene and two *clearly resolved bands* corresponding to the two isomers of guaiazulenediiron pentacarbonyl recovered in ca. 1:1 ratio. Elution with a gradually increasing ratio of benzene to hexane in the solvent mixture developed a brown band not seen in the previous reaction followed by the intense red band seen previously. Both bands yield oils upon removal of solvent but could be crystallized from pentane. The red solid gave an infrared spectrum showing two strong bands at 1990 and 1938 cm^{-1} with a weak band at 1895 cm^{-1}. The brown material shows a band at 1990 cm^{-1} (assignment questionable) and strong absorptions at 1943, 1875, and 1778 cm^{-1} each with a ^{13}C satellite (1900, 1840, and 1745 cm^{-1}, respectively), and this is almost certainly not a geometric isomer of the red material, which was recovered from both reactions. The thermal reaction of guaiazulenediiron pentacarbonyl with triethylphosphine in refluxing benzene for 24 h was investigated. Only a small amount of the red product was formed.

(Guaiazulene)$Ru_2(CO)_5$. $Ru_3(CO)_{12}$, 0.5 g, and guaiazulene, 0.5 g, were refluxed in 150 mL of toluene for 24 h. After removal of solvent the residue was taken up in hexane and chromatographed on a 15 × 2.5 cm column packed with alumina, activity grade III. Guaiazulene was eluted from the column first followed by a yellow band containing both isomers of (guaiazulene)$Ru_2(CO)_5$ (carbonyl bands at 2060, 2000, 1986, and 1942 cm^{-1}).

The mixture of isomers was enriched in ^{13}CO by irradiating 300 mg of the compound dissolved in 25 mL of CH_2Cl_2 under an atmosphere of CO enriched to 90% in ^{13}C for 24 h. The level of enrichment, ca. 15%, was determined by infrared spectrophotometry.

The separation of the two isomers was effected by chromato-

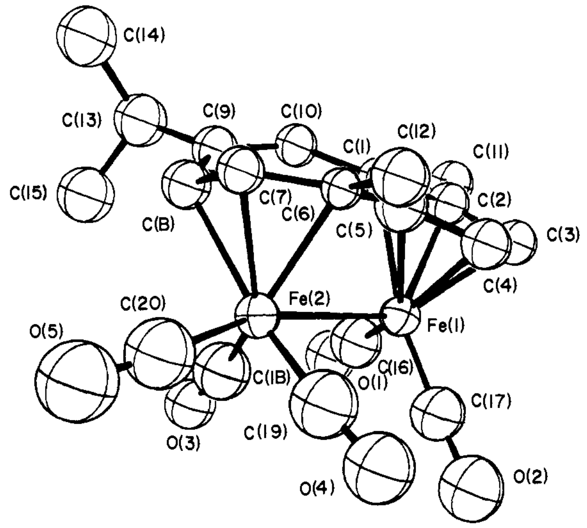

Figure 1. The molecular structure and atom numbering scheme for **1**, the first-eluted isomer of (guaiazulene)$Fe_2(CO)_5$. Atoms are represented by thermal vibration ellipsoids enclosing 50% of their election density.

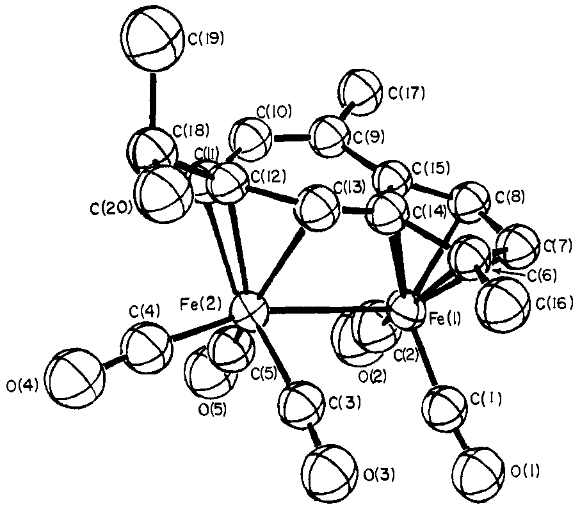

Figure 2. The molecular structure and atom numbering scheme (for molecule I) for **2**, the second-eluted isomer of (guaiazulene)$Fe_2(CO)_5$. Atoms are represented by thermal vibration ellipsoids enclosing 50% of their electron density.

Table I. Positional and Isotropic Temperature Parameters for $Fe_2(CO)_5$(Guaiazulene), Isomer 1, Molecule I

Atom	x	y	z	B_{iso}
O(1)	0.465 (2)	0.169 (2)	0.224 (3)	6.2 (8)
O(2)	0.567 (2)	0.407(2)	0.339 (3)	7.9 (9)
O(3)	0.406 (2)	0.817 (2)	0.442 (3)	4.8 (7)
O(4)	0.408 (2)	0.545 (2)	0.280 (3)	6.7 (8)
O(5)	0.623 (2)	0.301 (2)	0.020 (3)	8.3 (9)
C(1)	0.276 (2)	0.253 (2)	0.474 (4)	2.8 (9)
C(2)	0.262 (3)	0.272 (2)	0.320 (4)	3 (1)
C(3)	0.287 (3)	0.355 (2)	0.323 (4)	4 (1)
C(4)	0.323 (3)	0.387 (4)	0.486 (4)	4 (1)
C(5)	0.320 (4)	0.332 (4)	0.579 (4)	5 (1)
C(6)	0.346 (2)	0.343 (2)	0.747 (4)	2.4 (8)
C(7)	0.370 (2)	0.289 (2)	0.844 (4)	3.1 (9)
C(8)	0.386 (3)	0.203 (2)	0.774 (4)	4 (1)
C(9)	0.320 (3)	0.151 (2)	0.643 (4)	4 (1)
C(10)	0.270 (3)	0.172 (2)	0.513 (4)	3.4 (9)
C(11)	0.209 (3)	0.212 (2)	0.177 (4)	4 (1)
C(12)	0.338 (3)	0.428 (2)	0.837 (4)	4 (1)
C(13)	0.310 (3)	0.060 (2)	0.656 (4)	5 (1)
C(14)	0.260 (3)	0.047 (3)	0.800 (5)	6 (1)
C(15)	0.409 (3)	−0.027 (3)	0.657 (5)	6 (1)
C(16)	0.445 (3)	0.225 (4)	0.306 (4)	6 (1)
C(17)	0.502 (3)	0.362 (2)	0.378 (4)	5 (1)
C(18)	0.451 (3)	0.771 (2)	0.388 (5)	6 (1)
C(19)	0.448 (3)	0.612 (3)	0.278 (5)	7 (1)
C(20)	0.432 (3)	0.697 (3)	0.102 (5)	7 (1)

Table II. Positional and Isotropic Temperature Parameters for $Fe_2(CO)_5$(Guaiazulene), Isomer 1, Molecule II

Atom	x	y	z	B_{iso}
O(1)	1.095 (2)	0.364 (2)	1.008 (3)	7.0 (8)
O(2)	1.102 (2)	0.458 (2)	0.602 (3)	6.6 (8)
O(3)	1.122 (2)	0.223 (2)	0.778 (3)	5.9 (7)
O(4)	1.013 (2)	0.311 (2)	0.308 (3)	7.1 (8)
O(5)	1.014 (2)	0.070 (2)	0.366 (3)	8.0 (9)
C(1)	0.825 (2)	0.311 (2)	0.764 (3)	1.8 (8)
C(2)	0.847 (3)	0.396 (2)	0.845 (4)	5 (1)
C(3)	0.848 (3)	0.442 (2)	0.720 (5)	6 (1)
C(4)	0.834 (2)	0.387 (2)	0.580 (4)	2.9 (9)
C(5)	0.823 (3)	0.309 (2)	0.592 (4)	4 (1)
C(6)	0.796 (2)	0.239 (2)	0.475 (4)	2.8 (9)
C(7)	0.812 (2)	0.163 (2)	0.491 (4)	3.0 (9)
C(8)	0.850 (2)	0.138 (2)	0.637 (4)	2.3 (8)
C(9)	0.838 (2)	0.167 (2)	0.794 (4)	2.7 (9)
C(10)	0.818 (2)	0.241 (2)	0.852 (3)	1.4 (7)
C(11)	0.849 (3)	0.429 (2)	0.983 (4)	5 (1)
C(12)	0.754 (3)	0.250 (2)	0.689 (4)	4 (1)
C(13)	0.840 (3)	0.107 (3)	0.918 (5)	7 (1)
C(14)	0.941 (4)	0.076 (3)	0.950 (5)	9 (2)
C(15)	0.752 (4)	0.039 (3)	0.836 (6)	9 (2)
C(16)	1.041 (3)	0.363 (2)	0.886 (4)	5 (1)
C(17)	1.047 (3)	0.414 (3)	0.644 (5)	7 (1)
C(18)	1.049 (3)	0.220 (3)	0.681 (5)	7 (1)
C(19)	0.992 (3)	0.269 (2)	0.396 (4)	5 (1)
C(20)	0.989 (3)	0.134 (3)	0.425 (5)	6 (1)

graphing approximately 300 mg of the enriched mixture of the isomers on a 100 × 2.5 cm column packed with Woelm alumina, activity grade II, and eluting with hexane at 4 °C. The first yellow band collected is designated isomer 1 and the second as isomer 2.

Determination of Crystal Structures. $Fe_2(CO)_5$(Guaiazulene), Isomer 1. A crystal measuring 0.08 × 0.17 × 0.20 mm was mounted in a sealed capillary and examined on a Syntex $P\bar{1}$ four-circle automatic diffractometer equipped with a graphite-crystal, incident-beam monochromator. Many details of the crystallographic procedure have been reported elsewhere.[11] From the axial photographs 15 reflections of suitable intensity were chosen and computer centered. The setting angles for these reflections were used in the autoindexing program to select the best unit cell. The crystal was found to be triclinic. The following cell constants were obtained by least-squares refinement using 15 reflections collected in a 2θ range of 0–24.0°: a = 13.627 (7) Å, b = 16.993 (8) Å, c = 8.782 (3) Å, α = 98.78 (3)°, β = 99.79 (3)°, γ = 95.34 (4)°, V = 1965.6 (15) Å^3. The volume of the unit cell indicates the presence of four molecules in the unit cell, giving a calculated density of 1.521 g cm^{-1}. For the centric space group there would be two molecules per asymmetric unit. The widths at half-height for ω scans of several strong reflections were less than 0.25°.

Data were collected at 23 °C with Mo Kα radiation using the θ–2θ scan technique. The scan rate varied from 3 to 24° min^{-1} depending on the intensity of the reflection. A symmetric scan range 0.9° below Kα_1 to 0.9° above Kα_2 was used to measure 4507 unique reflections up to a maximum 2θ value of 43.0°. Of these, 1462 reflections with $F_o^2 > 2\sigma(F_o^2)$ were used to solve and refine the structure. Three standard reflections measured every 150 data points were stable showing no significant changes. The linear absorption coefficient for the compound is 15.42 cm^{-1} and no absorption correction was applied.

The Enraf-Nonius structure determination package (SDP) with a PDP 11/45 computer was used to solve and refine the structure.[12] The positions of the four iron atoms were obtained from an E-map

Table III. Positional and Anisotropic Temperature Parameters[a,b] for $Fe_2(CO)_5$(Guaiazulene), Isomer 1

Atom	x	y	z	β_{11}	β_{22}	β_{33}	β_{12}	β_{13}	β_{23}
				Molecule I					
Fe(1)	0.4129 (4)	0.3041 (3)	0.4155 (6)	41 (4)	30 (2)	108 (9)	6 (5)	22 (9)	24 (8)
Fe(2)	0.4898 (4)	0.3003 (3)	0.7309 (6)	42 (4)	32 (3)	61 (8)	2 (5)	7 (9)	6 (8)
				Molecule II					
Fe(1)	0.9609 (4)	0.3630 (3)	0.7196 (6)	63 (4)	20 (2)	139 (9)	6 (5)	53 (10)	41 (8)
Fe(2)	0.9535 (4)	0.2144 (4)	0.5321 (7)	56 (4)	41 (3)	111 (9)	17 (6)	51 (10)	27 (9)

[a] Temperature parameters were multiplied by 10^4. [b] Numbers in parentheses are estimated standard deviations in the least significant digit.

Table IV. Interatomic Distances (Å),[a,b] (Guaiazulene)$Fe_2(CO)_5$, Isomer I

Atoms	Distance	
	Molecule I	Molecule II
Fe(1)-Fe(2)	2.803 (7)	2.779 (7)
Fe(1)-C(16)	1.67 (4)	1.66 (4)
Fe(1)-C(17)	1.60 (4)	1.69 (4)
Fe(2)-C(18)	1.81 (4)	1.66 (4)
Fe(2)-C(19)	1.66 (4)	1.76 (4)
Fe(2)-C(20)	1.65 (4)	1.70 (4)
Fe(1)-C(1)	2.15 (3)	2.10 (3)
Fe(1)-C(2)	2.08 (3)	2.13 (3)
Fe(1)-C(3)	2.09 (3)	2.13 (4)
Fe(1)-C(4)	2.05 (3)	2.05 (3)
Fe(1)-C(5)	2.12 (3)	2.07 (3)
Fe(2)-C(5)	2.61 (3)	2.58 (3)
Fe(2)-C(6)	2.17 (3)	2.20 (3)
Fe(2)-C(7)	2.07 (3)	2.00 (3)
Fe(2)-C(8)	2.20 (3)	2.16 (3)
C(16)-O(1)	1.18 (4)	1.20 (4)
C(17)-O(2)	1.24 (4)	1.14 (4)
C(18)-O(3)	1.14 (4)	1.19 (4)
C(19)-O(4)	1.21 (4)	1.16 (4)
C(20)-O(5)	1.21 (4)	1.23 (4)
Distances for Atoms within the Guaiazulene Ring		
C(1)-C(2)	1.42 (3)	1.49 (4)
C(1)-C(5)	1.52 (4)	1.49 (4)
C(2)-C(3)	1.41 (4)	1.44 (4)
C(2)-C(11)	1.52 (2)	1.51 (4)
C(3)-C(4)	1.44 (4)	1.40 (4)
C(4)-C(5)	1.35 (4)	1.35 (4)
C(5)-C(6)	1.44 (4)	1.43 (4)
C(6)-C(12)	1.55 (4)	1.52 (3)
C(6)-C(7)	1.37 (3)	1.35 (4)
C(7)-C(8)	1.54 (4)	1.49 (3)
C(8)-C(9)	1.45 (4)	1.46 (3)
C(9)-C(13)	1.56 (4)	1.60 (4)
C(9)-C(10)	1.35 (4)	1.36 (3)
C(10)-C(1)	1.47 (4)	1.51 (3)
C(13)-C(14)	1.55 (4)	1.50 (5)
C(13)-C(15)	1.52 (4)	1.58 (5)

[a] Numbers in parentheses are the estimated standard deviations in the least significant figure. [b] Atoms are as labeled in Figure 1.

Table V. Bond Angles (deg), (Guaiazulene)$Fe_2(CO)_5$, Isomer 1

Atoms	Angle	
	Molecule I	Molecule II
Fe(2)-Fe(1)-C(16)	108 (1)	107 (1)
Fe(2)-Fe(1)-C(17)	99 (1)	98 (1)
Fe(1)-Fe(2)-C(18)	73 (1)	73 (1)
Fe(1)-Fe(2)-C(19)	83 (1)	85 (1)
Fe(1)-Fe(2)-C(20)	162 (1)	161 (1)
C(16)-Fe(1)-C(17)	91 (2)	93 (2)
C(18)-Fe(2)-C(19)	103 (2)	109 (2)
C(19)-Fe(2)-C(20)	87 (2)	86 (2)
C(18)-Fe(2)-C(20)	96 (2)	94 (3)
Fe(1)-C(16)-O(1)	177 (4)	176 (4)
Fe(1)-C(17)-O(2)	176 (3)	171 (4)
Fe(2)-C(18)-O(3)	170 (3)	174 (3)
Fe(2)-C(19)-O(4)	175 (4)	175 (3)
Fe(2)-C(20)-O(5)	177 (3)	171 (3)
Angles for Atoms within the Guaiazulene Ring		
C(2)-C(1)-C(10)	126 (3)	123 (3)
C(5)-C(1)-C(10)	128 (3)	128 (3)
C(2)-C(1)-C(5)	105 (3)	109 (3)
C(1)-C(2)-C(3)	111 (3)	105 (3)
C(1)-C(2)-C(11)	122 (3)	128 (3)
C(3)-C(2)-C(11)	126 (3)	127 (3)
C(2)-C(3)-C(4)	104 (3)	107 (3)
C(3)-C(4)-C(5)	114 (3)	116 (3)
C(4)-C(5)-C(1)	105 (3)	103 (3)
C(1)-C(5)-C(6)	125 (3)	125 (3)
C(4)-C(5)-C(6)	129 (3)	131 (3)
C(5)-C(6)-C(7)	130 (3)	127 (3)
C(5)-C(6)-C(12)	115 (3)	118 (3)
C(7)-C(6)-C(12)	114 (3)	115 (3)
C(6)-C(7)-C(8)	120 (3)	125 (3)
C(7)-C(8)-C(9)	126 (3)	124 (3)
C(8)-C(9)-C(10)	127 (3)	128 (3)
C(8)-C(9)-C(13)	115 (3)	118 (3)
C(10)-C(9)-C(13)	118 (3)	113 (3)
C(9)-C(10)-C(1)	126 (3)	123 (2)
C(9)-C(13)-C(15)	111 (3)	103 (3)
C(9)-C(13)-C(14)	110 (3)	112 (3)
C(14)-C(13)-C(15)	115 (3)	113 (3)

generated using the starting phase with the highest figure of merit from the program MULTAN based on 189 reflections with E values greater than 2.0. Three cycles of least-squares refinement on the four iron atoms gave discrepancy indices of: $R_1 = \Sigma\|F_o| - |F_c\|/\Sigma|F_o| = 0.314$ and $R_2 = [\Sigma w(|F_o| - |F_c|)^2/\Sigma w|F_o|^2]^{1/2} = 0.391$. Subsequent difference Fourier maps and least-squares cycles revealed the remaining 50 nonhydrogen atoms. The structure was refined by five full-matrix least-squares cycles to convergence with anisotropic thermal parameters for the iron atoms and isotropic ones for the remaining atoms to give the final discrepancy indices: $R_1 = 0.123$ and $R_2 = 0.114$. The error in an observation of the unit weight was 1.666. Further anisotropic refinement of the structure was not attempted due to the limited size and quality of the data set. Since the only important objective of this crystallographic investigation was to identify the structural configuration of the isomer, the somewhat high R values were considered acceptable.

No unusual trends were found in the data as a function of the various classes of Miller indices, reflection numbers, $\lambda^{-1} \sin \theta$, or $|F_o|$. A final difference Fourier map was found to be featureless. Anomalous scattering factors are from Cromer and Liberman.[13] Ordinary scattering factors were taken from Cromer and Waber.[14] A table of observed and calculated structure factors is available.[15]

Table VI. Positional and Thermal Parameters[a] and Their Estimated Standard Deviations for (Guaiazulene)$Fe_2(CO)_5$, Isomer 2

Atom	x	y	z	β_{11}	β_{22}	β_{33}	β_{12}	β_{13}	β_{23}
Fe1	0.8367 (2)	0.1236 (2)	0.2888 (2)	0.0075 (2)	0.0037 (1)	0.0066 (2)	0.0014 (3)	−0.0010 (4)	0.0002 (3)
Fe2	0.7400 (2)	0.0060 (2)	0.0923 (2)	0.0056 (2)	0.0040 (1)	0.0059 (2)	0.0006 (3)	−0.0008 (4)	0.0008 (3)
Fe3	0.1699 (2)	0.6668 (2)	0.2147 (2)	0.0078 (2)	0.0036 (1)	0.0068 (2)	0.0012 (3)	−0.0012 (4)	0.0010 (3)
Fe4	0.2627 (2)	0.5696 (2)	0.4111 (2)	0.0064 (2)	0.0039 (1)	0.0064 (2)	−0.0001 (3)	−0.0010 (4)	0.0008 (3)
O1	0.979 (1)	0.2793 (9)	0.188 (1)	6.0 (3)					
O2	0.665 (1)	0.2410 (11)	0.325 (1)	9.0 (4)					
O3	0.920 (1)	0.1179 (8)	−0.019 (1)	5.4 (3)					
O4	0.661 (1)	−0.0601 (9)	−0.157 (1)	5.9 (3)					
O5	0.581 (1)	0.1404 (9)	0.085 (1)	6.5 (3)					
O6	0.020 (1)	0.7791 (9)	0.313 (1)	5.8 (3)					
O7	0.333 (1)	0.8270 (10)	0.188 (1)	7.5 (4)					
O8	0.333 (1)	0.5229 (9)	0.660 (1)	6.4 (3)					
O9	0.073 (1)	0.6266 (9)	0.514 (1)	6.0 (3)					
O10	0.418 (1)	0.7410 (10)	0.422 (1)	7.5 (4)					
C1	0.914 (1)	0.219 (1)	0.226 (2)	4.4 (4)					
C2	0.734 (2)	0.193 (1)	0.310 (2)	6.5 (5)					
C3	0.850 (1)	0.075 (1)	0.032 (1)	3.9 (4)					
C4	0.690 (1)	−0.035 (1)	−0.054 (2)	4.5 (4)					
C5	0.649 (1)	0.090 (1)	0.095 (2)	4.6 (4)					
C6	0.964 (1)	0.039 (1)	0.320 (1)	3.4 (4)					
C7	0.961 (1)	0.098 (1)	0.426 (1)	3.8 (4)					
C8	0.856 (1)	0.075 (1)	0.468 (1)	3.7 (4)					
C9	0.675 (1)	−0.037 (1)	0.404 (1)	3.7 (4)					
C10	0.607 (1)	−0.080 (1)	0.313 (1)	3.9 (4)					
C11	0.632 (1)	−0.098 (1)	0.190 (1)	3.7 (4)					
C12	0.728 (1)	−0.134 (1)	0.154 (1)	3.1 (3)					
C13	0.838 (1)	−0.090 (1)	0.195 (1)	3.5 (4)					
C14	0.859 (1)	−0.022 (1)	0.296 (1)	3.4 (4)					
C15	0.792 (1)	0.001 (1)	0.389 (1)	3.3 (4)					
C16	1.063 (1)	0.036 (1)	0.250 (2)	4.8 (4)					
C17	0.639 (2)	−0.023 (1)	0.531 (2)	5.0 (4)					
C18	0.715 (1)	−0.222 (1)	0.072 (1)	3.8 (4)					
C19	0.694 (2)	−0.308 (1)	0.161 (2)	6.1 (5)					
C20	0.813 (1)	−0.233 (1)	−0.003 (2)	4.6 (4)					
C21	0.085 (1)	0.735 (1)	0.276 (2)	4.7 (4)					
C22	0.267 (2)	0.759 (1)	0.201 (2)	5.7 (5)					
C23	0.306 (1)	0.539 (1)	0.556 (2)	4.6 (4)					
C24	0.144 (1)	0.604 (1)	0.465 (2)	4.5 (4)					
C25	0.351 (2)	0.672 (1)	0.412 (2)	6.2 (5)					
C26	0.051 (1)	0.546 (1)	0.171 (1)	3.4 (4)					
C27	0.057 (1)	0.609 (1)	0.068 (2)	4.2 (4)					
C28	0.164 (1)	0.619 (1)	0.035 (1)	3.7 (4)					
C29	0.347 (1)	0.560 (1)	0.109 (2)	4.1 (4)					
C30	0.415 (1)	0.537 (1)	0.203 (1)	3.8 (4)					
C31	0.383 (1)	0.502 (1)	0.324 (2)	4.0 (4)					
C32	0.287 (1)	0.438 (1)	0.345 (1)	3.4 (4)					
C33	0.179 (1)	0.454 (1)	0.298 (1)	3.2 (4)					
C34	0.159 (1)	0.519 (1)	0.201 (1)	2.8 (3)					
C35	0.230 (1)	0.564 (1)	0.114 (1)	3.7 (4)					
C36	−0.052 (1)	0.517 (1)	0.234 (1)	3.8 (4)					
C37	0.398 (2)	0.598 (1)	−0.009 (2)	5.8 (5)					
C38	0.306 (2)	0.354 (1)	0.426 (2)	5.1 (4)					
C39	0.204 (2)	0.310 (1)	0.487 (2)	5.9 (5)					
C40	0.349 (2)	0.282 (2)	0.341 (2)	7.5 (6)					

[a] The form of the anisotropic thermal parameter is: $\exp[-(\beta_{11}h^2 + \beta_{22}k^2 + \beta_{33}l^2 + 2\beta_{12}hk + 2\beta_{13}hl + 2\beta_{23}hl)$.

$Fe_2(CO)_5$(Guaiazulene), Isomer 2. A crystal with dimensions of 0.31 × 0.18 × 0.16 mm was mounted in a sealed capillary. The orientation matrix and cell parameters were obtained in the same manner as described above. The crystal was found to be triclinic with a space group of $P\bar{1}$. The cell constants are: a = 12.286 (4) Å, b = 14.297 (3) Å, c = 11.029 (3) Å, α = 90.22 (2)°, β = 95.72 (2)°, γ = 97.54 (2)°, V = 1910.9 (82) Å^3. The volume indicates the presence of four molecules per unit cell, two molecules per asymmetric unit, with a calculated density for Z = 4 of 1.564 g cm^{-3}. The widths at half-height for ω scans of several strong reflections were 0.20°.

Data were collected at 23 °C in a manner identical with that employed for isomer 1; 4407 independent reflections were collected. Three standard reflections measured every 100 data points showed no significant deviation; 2050 reflections with $F_o^2 > 3\sigma(F_o^2)$ were used to solve and refine the structure.

The positions of the four iron atoms were obtained from an E-map generated using the starting phase with the highest figure of merit from the program MULTAN based on 468 reflections with E values greater than 1.65. Two cycles of least-squares refinement of the four iron atoms gave discrepancy indices of: $R_1 = \Sigma||F_o| - |F_c||/\Sigma|F_o| = 0.335$ and $R_2 = [\Sigma w(|F_o| - |F_c|)^2/\Sigma w|F_o|^2]^{1/2} = 0.414$. Subsequent difference Fourier maps and least-squares cycles revealed the 50 remaining atoms. The structure was refined with isotropic temperatures factors to discrepancy indices of R_1 = 0.080 and R_2 = 0.097. The iron atoms were then assigned anisotropic thermal parameters and two cycles of least squares led to a structure refinement with

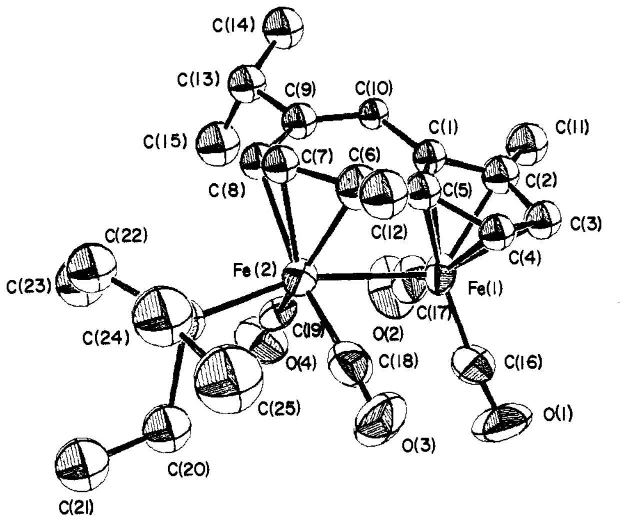

Figure 3. The molecular structure and atom numbering scheme for **5**. Atoms are represented by thermal vibration ellipsoids enclosing 50% of their electron density.

Table VII. Interatomic Distances (Å),[a,b] (Guaiazulene)$Fe_2(CO)_5$, Isomer 2

Atoms	Distance	
	Molecule I	Molecule II
Fe(1)-Fe(2)	2.810 (3)	2.806 (3)
Fe(1)-C(1)	1.74 (2)	1.70 (2)
Fe(1)-C(2)	1.74 (2)	1.67 (2)
Fe(2)-C(3)	1.76 (2)	1.72 (1)
Fe(2)-C(4)	1.74 (2)	1.76 (1)
Fe(2)-C(5)	1.75 (2)	1.71 (1)
Fe(1)-C(6)	2.10 (1)	2.13 (1)
Fe(1)-C(7)	2.11 (1)	2.11 (1)
Fe(1)-C(8)	2.10 (1)	2.09 (1)
Fe(1)-C(14)	2.14 (1)	2.10 (1)
Fe(1)-C(15)	2.11 (1)	2.09 (1)
Fe(2)-C(11)	2.21 (1)	2.17 (1)
Fe(2)-C(12)	2.11 (1)	2.08 (1)
Fe(2)-C(13)	2.19 (1)	2.16 (1)
Fe(2)-C(14)	2.62 (1)	2.59 (1)
C(1)-O(1)	1.20 (2)	1.18 (2)
C(2)-O(2)	1.18 (2)	1.20 (2)
C(3)-O(3)	1.18 (2)	1.18 (2)
C(4)-O(4)	1.19 (2)	1.14 (2)
C(5)-O(5)	1.16 (2)	1.19 (2)
Distances for Atoms within the Guaiazulene Ring		
C(6)-C(7)	1.44 (2)	1.45 (2)
C(6)-C(14)	1.46 (2)	1.44 (2)
C(6)-C(16)	1.51 (2)	1.51 (2)
C(7)-C(8)	1.41 (2)	1.39 (2)
C(8)-C(15)	1.46 (2)	1.44 (2)
C(9)-C(10)	1.33 (2)	1.33 (2)
C(9)-C(17)	1.54 (2)	1.57 (2)
C(9)-C(15)	1.49 (2)	1.45 (2)
C(10)-C(11)	1.45 (2)	1.50 (2)
C(11)-C(12)	1.44 (2)	1.43 (2)
C(12)-C(13)	1.44 (2)	1.42 (2)
C(12)-C(18)	1.53 (2)	1.54 (2)
C(13)-C(14)	1.45 (2)	1.45 (2)
C(14)-C(15)	1.43 (2)	1.45 (2)
C(18)-C(19)	1.58 (2)	1.54 (2)
C(18)-C(20)	1.56 (2)	1.56 (2)

[a] Numbers in parentheses are the estimated standard deviations in the least significant figure. [b] Atoms are as labeled in Figure 2.

Table VIII. Bond Angles (deg), (Guaiazulene)$Fe_2(CO)_5$, Isomer 2

Atoms	Angle	
	Molecule I	Molecule II
Fe(2)-Fe(1)-C(1)	106 (1)	105 (1)
Fe(2)-Fe(1)-C(2)	102 (1)	103 (1)
Fe(1)-Fe(2)-C(3)	162 (1)	162 (1)
Fe(1)-Fe(2)-C(4)	76 (1)	76 (1)
Fe(1)-Fe(2)-C(5)	77 (1)	77 (1)
Fe(1)-C(1)-O(1)	172 (1)	175 (1)
Fe(1)-C(2)-O(2)	179 (1)	177 (1)
Fe(2)-C(3)-O(3)	173 (1)	175 (1)
Fe(2)-C(4)-O(4)	176 (1)	172 (1)
Fe(2)-C(5)-O(5)	172 (1)	174 (1)
C(1)-Fe(1)-C(2)	90 (1)	93 (1)
C(3)-Fe(2)-C(4)	90 (1)	90 (1)
C(3)-Fe(2)-C(5)	99 (1)	104 (1)
C(4)-Fe(2)-C(5)	94 (1)	95 (1)
Angles for Atoms within the Guaiazulene Ring		
C(16)-C(6)-C(7)	125 (1)	125 (1)
C(16)-C(6)-C(14)	125 (1)	128 (1)
C(7)-C(6)-C(14)	109 (1)	107 (1)
C(6)-C(7)-C(8)	107 (1)	109 (1)
C(7)-C(8)-C(15)	108 (1)	109 (1)
C(8)-C(15)-C(14)	109 (1)	107 (1)
C(8)-C(15)-C(9)	123 (1)	124 (1)
C(15)-C(14)-C(6)	106 (1)	108 (1)
C(15)-C(14)-C(13)	132 (1)	131 (1)
C(15)-C(9)-C(10)	123 (1)	124 (1)
C(15)-C(9)-C(17)	115 (1)	117 (1)
C(17)-C(9)-C(10)	122 (1)	119 (1)
C(9)-C(10)-C(11)	127 (1)	127 (1)
C(10)-C(11)-C(12)	126 (1)	126 (1)
C(11)-C(12)-C(13)	122 (1)	122 (1)
C(11)-C(12)-C(18)	120 (1)	116 (1)
C(13)-C(12)-C(18)	118 (1)	121 (1)
C(12)-C(13)-C(14)	122 (1)	123 (1)
C(13)-C(14)-C(6)	122 (1)	121 (1)
C(12)-C(18)-C(19)	105 (1)	104 (1)
C(12)-C(18)-C(20)	116 (1)	115 (1)
C(19)-C(18)-C(20)	111 (1)	113 (1)
C(14)-C(15)-C(9)	128 (1)	128 (1)

convergence at final R factors of 0.068 and 0.085 and an error in an observation of unit weight of 1.56. A final difference map was judged to be free of significant features. No unusual trends were observed in an analysis of $\Sigma w(|F_o| - |F_c|)^2$ as a function of $|F_o|$, reflection number, $\lambda^{-1} \sin \theta$, or various classes of indices. A table of observed and calculated structure factor amplitudes is available.[15]

$Fe_2(CO)_4P(Et)_3$(Guaiazulene). A crystal measuring 0.15 × 0.23 × 0.30 mm was mounted in a sealed capillary. The orientation matrix and cell parameters were obtained in the same manner as described for the two previous structures. The crystal was found to be monoclinic with a space group of $P2_1/n$ determined from systematic absences. The cell constants are a = 12.487 (5) Å, b = 13.918 (5) Å, c = 15.196 (6) Å, β = 103.90 (3)°, and V = 2563.6 (16) Å^3. For Z = 4 the calculated density is 1.399 g/cm^{-3}. The widths at half-height for ω scans of several intense reflections were 0.20°.

Data were collected at 23 °C in the same manner as that for the $(C_{15}H_{18})Fe_2(CO)_5$ isomers; 3366 unique reflections within a 2θ range of 0 to 45° were collected. Of these, 1107 reflections with $F_o^2 > 3\sigma(F_o^2)$ were used to solve and refine the crystal structure. Three standard reflections measured every 200 data points showed no trends or significant changes.

The positions of the two iron atoms were obtained from a three-dimensional Patterson map.[16] Subsequent least-squares cycles and difference Fourier maps revealed the rest of the nonhydrogen atoms. Full-matrix least-squares refinement with anisotropic temperature factors for the iron atoms, the eight atoms of the carbonyl groups and the phosphorus atom and isotropic temperature parameters for remaining 21 carbon atoms converged in four cycles to give the final discrepancy indices of R_1 = 0.075 and R_2 = 0.085. The error in an observation of the unit weight was 1.642.

No unusual trends were found in the data as a function of the various classes of Miller indices, reflection number, $\lambda^{-1} \sin \theta$, or $|F_o|$. Scattering tables used for the atoms were those used in the previous

Table IX. Positional and Anisotropic Temperature Parameters[a,b] for $Fe_2(CO)_4P(C_2H_5)_3$(Guaiazulene)

Atom	x	y	z	β_{11}	β_{22}	β_{33}	β_{12}	β_{13}	β_{23}
Fe(1)	0.0206 (3)	0.0112 (2)	0.2473 (2)	50 (3)	50 (3)	43 (2)	4 (2)	0 (2)	−7 (2)
Fe(2)	−0.1899 (2)	0.0682 (2)	0.2608 (2)	52 (3)	45 (2)	41 (2)	4 (2)	9 (2)	3 (2)
P	−0.3565 (5)	0.0689 (5)	0.2865 (4)	59 (5)	55 (5)	60 (4)	9 (5)	27 (4)	6 (4)
O(1)	0.0709 (17)	−0.1671 (13)	0.3404 (14)	190 (26)	46 (13)	116 (17)	−7 (16)	−6 (15)	31 (13)
O(2)	−0.0324 (15)	−0.0791 (15)	0.0730 (12)	121 (19)	132 (19)	73 (13)	−3 (15)	28 (13)	−44 (13)
O(3)	−0.1209 (15)	−0.0586 (15)	0.4179 (13)	117 (20)	138 (21)	78 (15)	32 (16)	24 (14)	63 (14)
O(4)	−0.1551 (14)	−0.0751 (12)	0.1192 (12)	129 (19)	59 (13)	79 (14)	−22 (14)	30 (13)	−28 (11)
C(16)	0.0446 (22)	−0.0970 (20)	0.3003 (19)	102 (28)	43 (21)	91 (24)	31 (20)	25 (19)	0 (18)
C(17)	−0.0108 (20)	−0.0389 (18)	0.1440 (21)	77 (25)	61 (22)	83 (22)	22 (17)	24 (20)	−16 (17)
C(18)	−0.1456 (20)	−0.0101 (21)	0.3583 (18)	78 (24)	78 (23)	60 (19)	−24 (22)	2 (18)	8 (19)
C(19)	−0.2250 (18)	−0.0160 (17)	0.1737 (17)	72 (22)	19 (17)	66 (18)	16 (17)	17 (16)	−4 (15)

[a] Temperature factors were multiplied by 10^4. [b] Numbers in parentheses are the estimated standard deviations in the least significant digit.

Table X. Positional and Isotropic Temperature Parameters for $Fe_2(CO)_4P(C_2H_5)_3$(Guaiazulene)

Atom	x	y	z	B_{iso}
C(1)	0.031 (2)	0.154 (2)	0.209 (2)	3.0 (5)
C(2)	0.136 (2)	0.108 (2)	0.220 (2)	3.8 (5)
C(3)	0.173 (2)	0.076 (2)	0.310 (1)	3.6 (5)
C(4)	0.090 (2)	0.101 (1)	0.356 (1)	3.1 (5)
C(5)	−0.001 (2)	0.152 (2)	0.297 (1)	3.4 (5)
C(6)	−0.095 (2)	0.190 (2)	0.322 (2)	4.6 (6)
C(7)	−0.192 (2)	0.217 (1)	0.260 (1)	3.2 (4)
C(8)	−0.217 (2)	0.187 (1)	0.165 (1)	3.3 (5)
C(9)	−0.145 (2)	0.202 (1)	0.104 (1)	3.3 (5)
C(10)	−0.033 (2)	0.193 (1)	0.122 (1)	2.4 (4)
C(11)	0.202 (2)	0.106 (2)	0.147 (2)	5.1 (6)
C(12)	−0.075 (2)	0.220 (2)	0.423 (2)	4.8 (6)
C(13)	−0.209 (2)	0.232 (2)	0.005 (2)	4.0 (5)
C(14)	−0.136 (2)	0.276 (2)	−0.051 (2)	4.9 (6)
C(15)	−0.267 (2)	0.142 (2)	−0.042 (2)	5.7 (6)
C(20)	−0.408 (2)	−0.054 (2)	0.300 (2)	5.4 (6)
C(21)	−0.526 (2)	−0.058 (2)	0.316 (2)	6.3 (7)
C(22)	−0.471 (2)	0.127 (2)	0.203 (2)	5.6 (6)
C(23)	−0.498 (2)	0.072 (2)	0.112 (2)	6.1 (6)
C(24)	−0.381 (2)	0.134 (2)	0.388 (2)	7.1 (7)
C(25)	−0.312 (2)	0.088 (2)	0.481 (2)	8.9 (8)

structures.[13,14] A table of observed and calculated structure factors is available.[15]

Results

Crystal Structures. Compound **1** is found to be the isomer of (guaiazulene)$Fe_2(CO)_5$ in which the isopropyl substituent is *not* attached to the three carbon atoms bound to the $Fe(CO)_3$ group. Overall, the structure closely resembles that of (azulene)$Fe_2(CO)_5$.[17] It is shown in Figure 1, which gives the numbering scheme. Tables I–III give the positional and thermal parameters of all atoms. Tables IV and V present bond distances and bond angles, respectively.

Compound **2** is the other isomer of (guaiazulene)$Fe_2(CO)_5$ and its structure is shown in Figure 2. Atomic coordinates and thermal parameters are given in Table VI, and the bond distances and angles are given in Tables VII and VIII. For simplicity in Tables VII and VIII only the atoms of molecule I are listed by number. Iron atoms Fe(3) and Fe(4) of molecule II correspond to Fe(1) and Fe(2) of molecule **1**, oxygen atoms O(n + 5) and carbon atoms C(n + 20) are those in molecule **2** that correspond to O(n) and C(n) of molecule **1**.

Compound **5** is the PEt_3 derivative of **1**, as shown in Figure 3. Positional and thermal parameters are presented in Tables IX and X and the interatomic distances and angles in Tables XI and XII.

Table XI. Interatomic Distances (Å)[a,b] in (Guaiazulene)-$Fe_2(CO)_4P(C_2H_5)_3$

Atoms	Distance	Atoms	Distance
Fe(1)–Fe(2)	2.800 (4)	Fe(2)–P	2.207 (7)
Fe(1)–C(16)	1.70 (3)	Fe(2)–C(18)	1.81 (3)
Fe(1)–C(17)	1.68 (3)	Fe(2)–C(19)	1.74 (2)
Fe(1)–C(1)	2.08 (2)	Fe(2)–C(7)	2.07 (2)
Fe(1)–C(2)	2.09 (2)	Fe(2)–C(8)	2.19 (2)
Fe(1)–C(3)	2.12 (2)	Fe(2)–C(6)	2.15 (2)
Fe(1)–C(4)	2.09 (2)	Fe(2)–C(5)	2.57 (2)
Fe(1)–C(5)	2.14 (2)	C(18)–O(3)	1.16 (3)
C(16)–O(1)	1.11 (2)	C(19)–O(4)	1.19 (3)
C(17)–O(2)	1.16 (2)	C(20)–C(21)	1.55 (3)
P–C(20)	1.86 (2)	C(22)–C(23)	1.55 (3)
P–C(22)	1.86 (2)	C(24)–C(25)	1.60 (3)
P–C(24)	1.88 (3)		
Distances for Atoms within the Guaiazulene Ring			
C(1)–C(2)	1.43 (2)	C(2)–C(11)	1.53 (3)
C(1)–C(5)	1.48 (2)	C(2)–C(3)	1.42 (2)
C(3)–C(4)	1.42 (2)	C(4)–C(5)	1.45 (2)
C(5)–C(6)	1.42 (3)	C(6)–C(7)	1.39 (2)
C(6)–C(12)	1.55 (3)	C(7)–C(8)	1.45 (2)
C(8)–C(9)	1.45 (2)	C(9)–C(13)	1.58 (2)
C(9)–C(10)	1.36 (2)	C(13)–C(14)	1.52 (2)
C(10)–C(1)	1.48 (2)	C(13)–C(15)	1.53 (3)

[a] Numbers in parentheses are the estimated standard deviations in the least significant digits. [b] Atoms are labeled as in Figure 3.

In all three structures, the packing of the molecules showed no unusual intermolecular contacts. The agreement between corresponding dimensions of the two independent molecules in the crystals of **1** and **2** is uniformly good.

Carbon-13 NMR Spectra. The spectra for **1** and **2** from −131 to 80 °C are shown in Figures 4 and 5. The spectrum at −131 °C and probably also the one at −100 °C for **2** show viscosity broadening. Even at these low temperatures the slow exchange limit for **2** was not observed; already the three lines due to CO groups in the $Fe(CO)_3$ group had collapsed, and at −90 °C the signal arising at 27.0 ppm is the average for all three of these CO groups. In **1** on the other hand the signals for all five CO ligands can be seen, albeit somewhat viscosity-broadened, at −131 °C. It is quite evident the spectra for **1** and **2** are qualitatively similar. They differ somewhat in the relative chemical shifts and in the fact that both averaging processes occur at slightly lower temperatures for **2** than for **1**.

For compounds **3** and **4**, the ruthenium analogues of **1** and **2**, respectively, the carbon-13 spectra are given in Figures 6 and 7. The most important difference between the iron and ruthenium compounds from a practical point of view is that the isomer interconversion, $\mathbf{3} \rightleftharpoons \mathbf{4}$, is far more facile than $\mathbf{1} \rightleftharpoons$

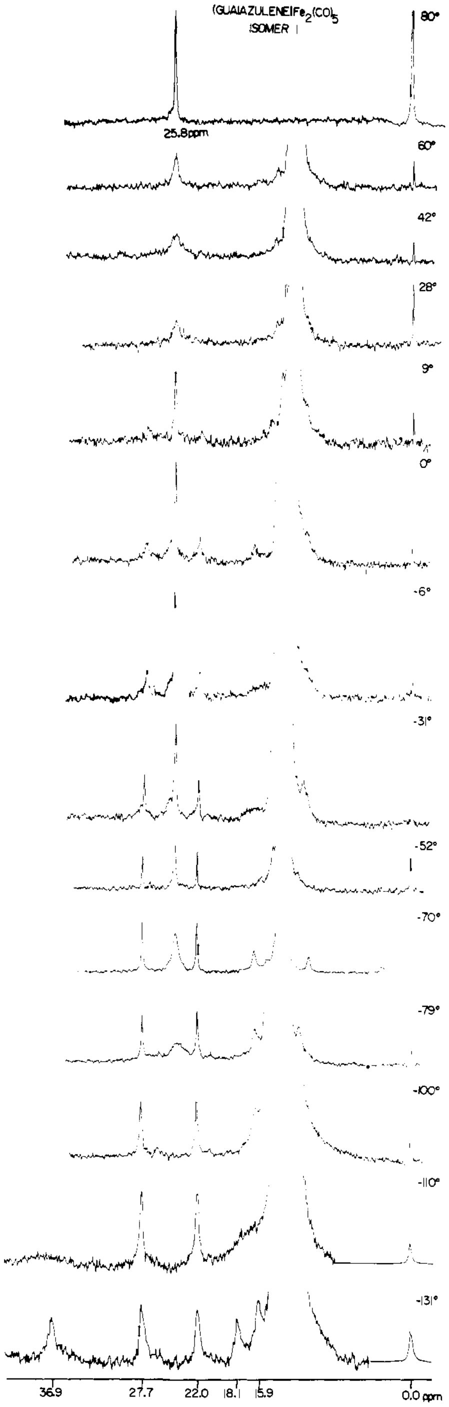

Figure 4. Carbon-13 NMR spectra for **1** in the CO region. Chemical shifts are in parts per million downfield from internal CS_2, which is responsible for the peak at the extreme right. The very large peak at ca. 13 ppm is the carbonyl carbon atom of acetone. The five peaks due to CO ligands of 1 are those whose chemical shifts are given in the spectrum at −131 °C.

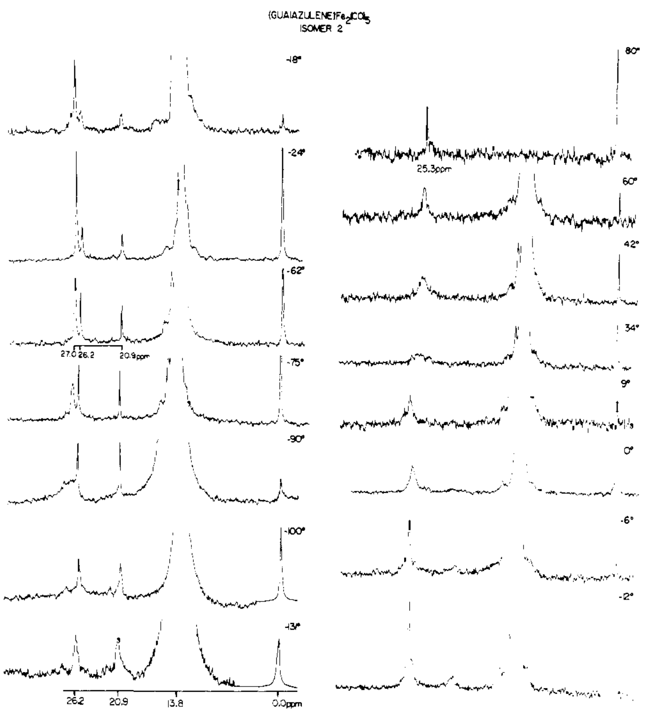

Figure 5. Carbon-13 NMR spectra for **2**, in the CO region. The large peak at 13.8 ppm is due to solvent acetone and the peak at the extreme right is due to CS_2. Chemical shifts are given in parts per million downfield from CS_2.

Table XII. Bond Angles (deg), (Guaiazulene)$Fe_2(CO)_4P(C_2H_5)_3$

Atoms	Angle	Atoms	Angle
Fe(2)-Fe(1)-C(16)	106 (1)	Fe(1)-Fe(2)-C(18)	77.4 (8)
Fe(2)-Fe(1)-C(17)	100.0 (8)	Fe(1)-Fe(2)-C(19)	79.8 (7)
C(16)-Fe(1)-C(17)	92 (1)	Fe(1)-Fe(2)-P	162.8 (2)
Fe(1)-C(16)-O(1)	173 (2)	C(18)-Fe(2)-C(19)	100 (1)
Fe(1)-C(17)-O(2)	176 (3)	C(18)-Fe(2)-P	88.4 (8)
Fe(2)-C(18)-O(3)	178 (2)	C(19)-Fe(2)-P	93.5 (8)
Fe(2)-C(19)-O(4)	174 (2)	P-C(20)-C(21)	114 (2)
Fe(2)-P-C(20)	112.4 (8)	P-C(22)-C(23)	111 (2)
Fe(2)-P-C(22)	118.8 (8)	P-C(24)-C(25)	112 (2)
Fe(2)-P-C(24)	119.6 (8)		
Angles for Atoms within the Guaiazulene Ring			
C(10)-C(1)-C(2)	123 (2)	C(1)-C(2)-C(11)	124 (2)
C(1)-C(2)-C(3)	109 (2)	C(3)-C(2)-C(11)	125 (2)
C(2)-C(3)-C(4)	107 (2)	C(3)-C(4)-C(5)	112 (2)
C(4)-C(5)-C(1)	103 (2)	C(4)-C(5)-C(6)	127 (2)
C(1)-C(5)-C(6)	131 (2)	C(5)-C(6)-C(12)	114 (2)
C(5)-C(6)-C(7)	124 (2)	C(7)-C(6)-C(12)	120 (2)
C(6)-C(7)-C(8)	122 (2)	C(7)-C(8)-C(9)	125 (2)
C(8)-C(9)-C(10)	129 (2)	C(8)-C(9)-C(13)	113 (2)
C(10)-C(9)-C(13)	118 (2)	C(9)-C(10)-C(1)	121 (2)
C(9)-C(13)-C(14)	114 (2)	C(9)-C(13)-C(15)	108 (2)
C(14)-C(13)-C(15)	110 (2)		

2. Therefore, while the spectra of the iron compounds were obtainable, even up to 80 °C, without any observable complications from isomerization, the spectra of the ruthenium analogues are more complex because the set of spectra for each one of the isomers contains peaks, whose intensities increase with time and temperature, due to contamination by the other isomer.

In Figure 6, the five main peaks whose chemical shifts are specified below the −85 °C spectrum are those of compound **3** (isomer 1 of $C_{15}H_{18}Ru_2(CO)_5$) but additional, weaker peaks are evident, and the fact that they are due to the presence of **4** (isomer 2), that forms even during the workup, is clear by comparison[18] with Figure 7. It is evident that the behavior of **3** parallels that of **1**, with the signals for the $M(CO)_3$ group collapsing and coalescing while those for the $M(CO)_2$ group remain separate and sharp. As in the previous comparison of the azulene complexes of iron and ruthenium, the latter have a higher activation energy. While the coalescence temperature, T_c, for $Fe(CO)_3$ in **1** is around −110 °C, T_c for the $Ru(CO)_3$ group in **3** is around −40 °C. Similarly, for **2** the T_c for $Fe(CO)_3$ is about −100 °C while that for $Ru(CO)_3$ in **4** is about −50 °C.

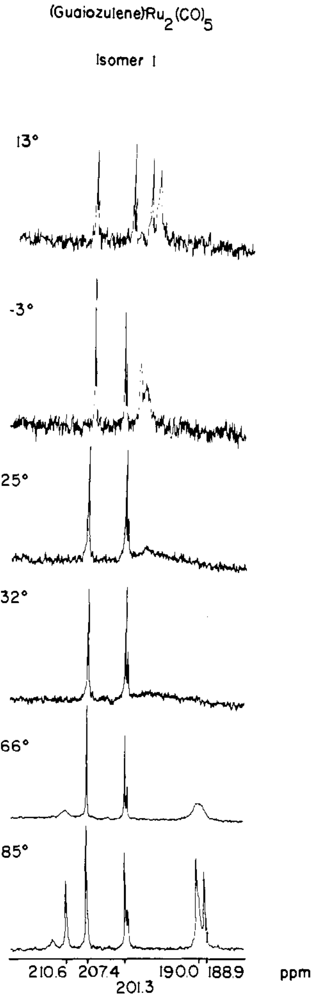

Figure 6. Carbon-13 NMR spectra for **3** (isomer 1 of (guaiazulene)-$Ru_2(CO)_5$). At each temperature weaker peaks due to the presence of some of isomer 2 may be seen.

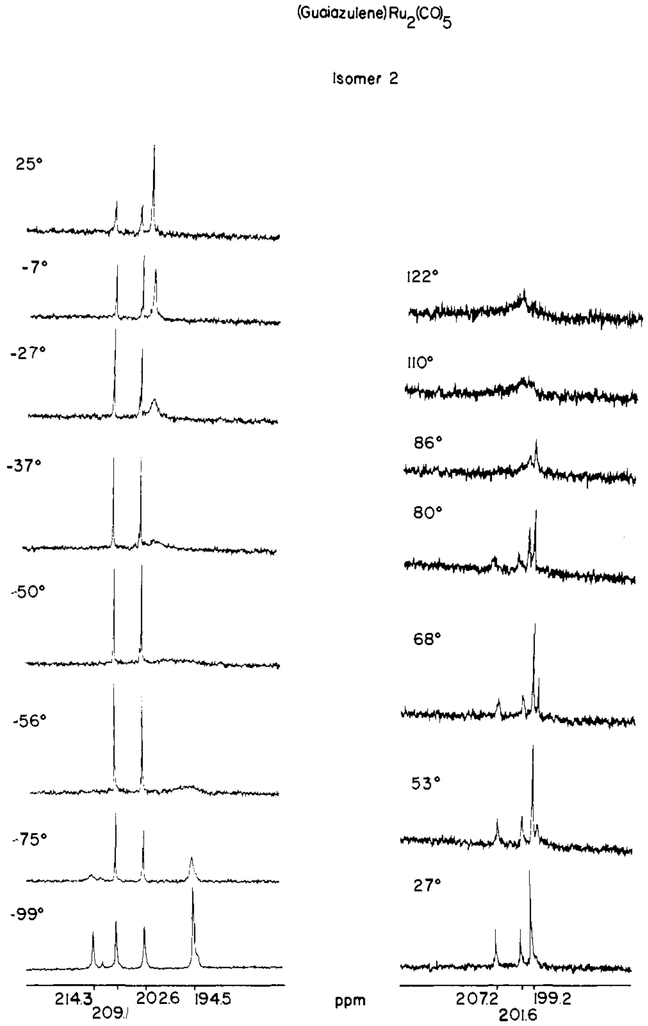

Figure 7. Carbon-13 NMR spectra for **4** (isomer 2 of (guaiazulene)-$Ru_2(CO)_5$). Contamination by **3** (isomer 1) can be observed in several spectra and especially above 50 °C. At about 80 °C the sample is essentially an equilibrium mixture of the two isomers.

Collapse of the $Fe(CO)_2$ signals in both **1** and **2** begins below 0 °C whereas in **3** and **4** the required temperature is much higher. The process has not actually been seen in **3** but can be seen to begin above about 50 °C in **4**. Unfortunately isomer interconversion and/or decomposition in **3** and **4** make it impossible to obtain clean spectra in the fast exchange limit for the individual isomers.

Even though the rate of interconversion of **3** and **4** is rapid enough to make it virtually impossible to obtain completely pure solutions of separate isomers and to give, over the experimental time periods involved, an equilibrium mixture of isomers at higher temperatures (see the 80 °C spectrum in Figure 7) the rate of isomer interconversion, $\mathbf{3} \rightleftharpoons \mathbf{4}$, does not become fast on the NMR time scale. This was demonstrated by observing the signals from the guaiazulene rings. Even at 122 °C, separate sets of sharp signals for the two isomers are observed.

The carbon-13 spectra for compound **5** are shown in Figure 8. These show that both CO groups of the $Fe(CO)_2$ unit and *one* of those on the $Fe(CO)_2PEt_3$ unit become involved in rapid exchange beginning about 40 °C while the other CO group in the $Fe(CO)_2PEt_3$ group continues to give a sharp doublet even at 95 °C.

The fact that only one isomer of (guaiazulene)Fe_2-$(CO)_4PEt_3$, **5**, is isolated regardless of which isomer, **1** or **2**, of (guaiazulene)$Fe_2(CO)_5$ is used as the starting material in the photochemical reactions has a plausible explanation (Scheme I). We propose that the initial step is photodissociation of one CO group from the $Fe(CO)_3$ moiety to give an intermediate that has an essentially symmetrical structure. While the unsymmetrical disposition of substituents on the ring system disallows the attainment of a rigorously symmetrical intermediate, the situation is similar to that with (guaiazulene)-$Mo_2(CO)_6$ where the distortion is very slight. As this intermediate captures PEt_3, steric factors steer the system continuously toward the arrangement in which there is least non-

Scheme I

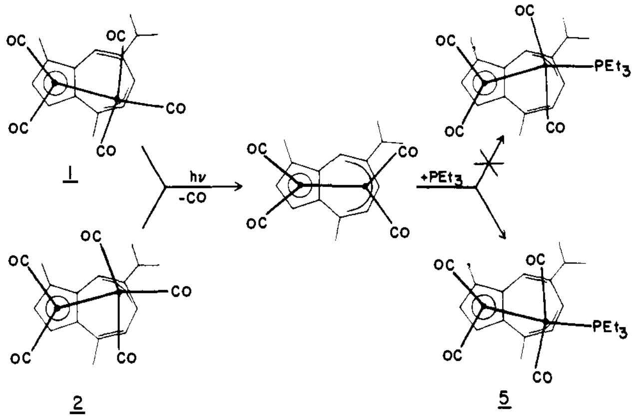

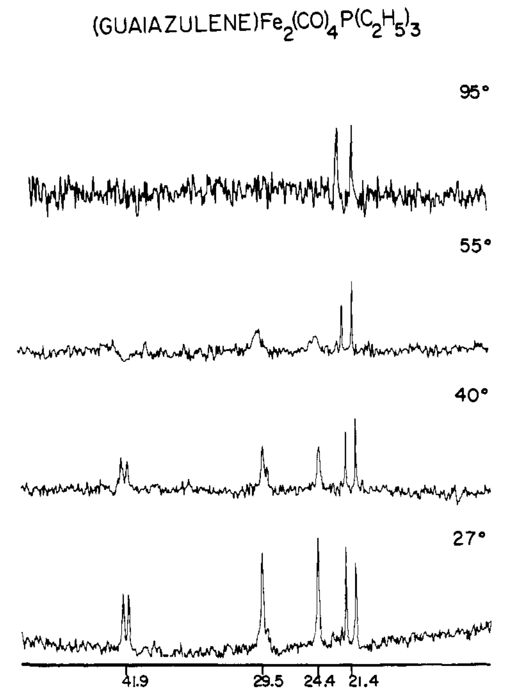

Figure 8. Carbon-13 NMR spectra of compound **5**. The splitting of the signals at 41.9 and 21.4 ppm is due to ^{31}P coupling and identifies them as belonging to the CO ligands in the $Fe(CO)_2PEt_3$ group.

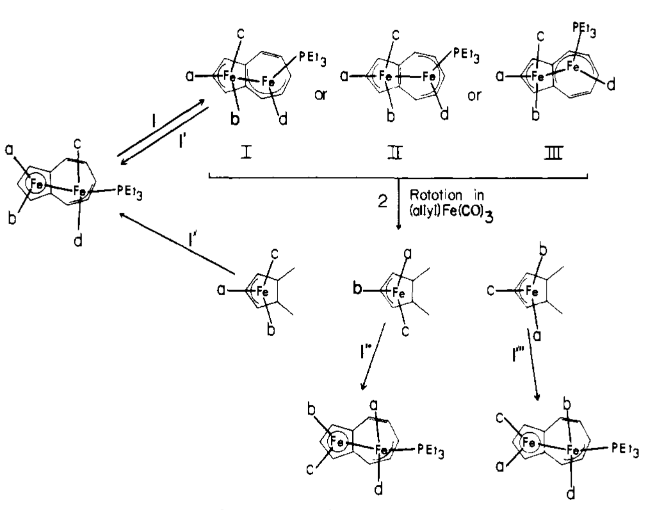

Figure 9. The proposed pathway for internuclear CO exchange in (guaiazulene)$Fe_2(CO)_4PEt_3$, compound **5**.

bonded repulsion, namely, to the sterically favored product, **5**.

Discussion

The structural identities of compounds **1** and **2** have been unambiguously established. They are, as expected, the isomers originally anticipated by Burton, Pratt, and Wilkinson. Their carbonyl scrambling processes are very similar to each other and to the corresponding processes in (azulene)$Fe_2(CO)_5$. There are only small quantitative differences. Thus, the general pattern of behavior in all compounds of the type $XM_2(CO)_5$, whether X is azulene or guaiazulene, is qualitatively invariant and the quantitative differences are small. The change from Fe to Ru causes an increase in the activation energies for carbonyl scrambling but lowers the activation energy for the interconversion of the isomers when X = guaiazulene.

It was emphasized previously in our report on the (azulene)$M_2(CO)_5$ compounds that there are a number of permutation schemes, and, hence, motional pathways, for CO ligands, that might account for the observation of complete scrambling of all CO groups at higher temperatures and that the observed line shape changes could not distinguish among them. The spectra of the (guaiazulene)$M_2(CO)_5$ molecules do not resolve the problem. However, the remarkably selective scrambling observed for (guaiazulene)$Fe_2(CO)_4PEt_3$, compound **5**, is highly significant. It prompts us to propose a pathway for exchange not only in **5** itself but in all of the $XM_2(CO)_5$ compounds in which X = azulene or guaiazulene. This pathway is shown in Figure 9.

In step 1, the CO ligand labeled c shifts to the left iron atom. This motion is accompanied by a reorganization of the π electron density of the guaiazulene system (the appended methyl and isopropyl groups are omitted in Figure 9 for clarity) so that an allyl moiety is made available to the new $Fe(CO)_3$ group and a pentadienyl moiety to the new $Fe(CO)PEt_3$ group. There are at least three plausible ways, I, II, and III, to write such an intermediate; we see no objective basis for choosing among them for compound **5** itself (but vide infra) nor is such a choice necessary to the thrust of our argument.

It must also be pointed out that the movement of c to the left iron atom rather than d is purely arbitrary. The experimental results require that it be either one or the other and not both that can do this, but until we know how to assign the spectrum we cannot say which one moves. This point also is not essential to the thrust of our argument since an exactly analogous mechanism could be written in which d shifts rather than c.

Once an intermediate of the type I, II, or III is formed, at the relatively high temperature we are dealing with in step 2, scrambling of the CO groups in the $Fe(CO)_3$ group (probably, but not necessarily, by rigid rotation) may be expected to occur rapidly.[19-26] Microscopic reversibility then demands that restoration of the initial structure occur only by one of the steps 1′, 1″, or 1‴. In this way each of the carbonyl groups, a, b, and c, has access to each of the three positions initially occupied by them whereas carbonyl group d can never stray from its initial site.

An intermediate of type II, Figure 9, while possible in principle for compound **5** can probably be ruled out here because such an intermediate *must* be ruled out for compounds **1** and **2**. For these $Fe_2(CO)_5$ species such an intermediate would provide a pathway for interconversion of **1** and **2** allowing interconversion to occur at the same rate as total scrambling of CO groups. This is not observed. An intermediate of type II also suffers from the requirement that either the Fe-Fe distance be extended (compared to that in the ground state) or that the essentially planar bicycloolefin buckle. It is possible, however, that an intermediate like II may be more accessible in the case of the ruthenium analogues, **3** and **4**, since the Ru-Ru bond is likely to be ca. 0.2 Å longer. This may be the way to explain the much greater ease of interconversion of the isomers **3** and **4**.

The final point to be dealt with is the applicability of this sort of pathway to the molecules **1–5**, **12**, and **13** only but not to the others mentioned, namely, **6–11**, in which no internuclear scrambling has been observed. For species **7–11** the shift of a single CO from one metal atom to the other would produce a very improbable intermediate, not likely to be thermally accessible, nor to be capable of rapid local scrambling in the $M(CO)_4$ or $M(CO)_2$ groups even if formed. In the case of **6**, which is formally similar to the azulene and guaiazulene systems containing $Fe_2(CO)_5$, there is no acceptable way to rearrange the π electron density to stabilize an intermediate in which a CO group of the $Fe(CO)_3$ unit has shifted to the other iron atom.

Acknowledgments. Financial support was provided by the National Science Foundation (Grant No. 33142X) and by the

Robert A. Welch Foundation (Grant No. A494). We thank Dr. Douglas L. Hunter for assistance and also the staff of the Molecular Structure Corporation for guidance and assistance in the use of their facilities.

Supplementary Material Available: Tables of structure factor amplitudes (24 pages). See any current masthead page for ordering instructions.

References and Notes

(1) P.L. thanks the Program for Cultural Exchange between the United States of America and Spain for financial aid during a leave of absence from the University of Zaragoza.

(2) F. A. Cotton, D. L. Hunter, and P. Lahuerta, *Inorg. Chem.*, **14**, 511 (1975).

(3) F. A. Cotton, D. L. Hunter, and P. Lahuerta, *J. Am. Chem. Soc.*, **97**, 1046 (1975).

(4) F. A. Cotton and D. L. Hunter, *J. Am. Chem. Soc.*, **97**, 5739 (1975).

(5) F. A. Cotton, D. L. Hunter, and P. Lahuerta, *J. Organomet. Chem.*, **87**, C42 (1975).

(6) F. A. Cotton, P. Lahuerta, and B. R. Stults, *Inorg. Chem.*, **15**, 1866 (1976).

(7) F. A. Cotton and B. E. Hanson, *Inorg. Chem.*, **15**, 2806 (1976).

(8) F. A. Cotton, B. E. Hanson, J. R. Kolb, and P. Lahuerta, *Inorg. Chem.*, **16**, 89 (1977).

(9) D. F. Shriver, "The Manipulation of Air-Sensitive Compounds", McGraw-Hill, New York, N.Y., 1969, Chapter 7.

(10) R. Burton, L. Pratt, and G. Wilkinson, *J. Chem. Soc.*, 4290 (1960).

(11) F. A. Cotton, B. A. Frenz, G. Deganello, and A. Shaver, *J. Organomet. Chem.*, **50**, 227 (1973).

(12) Computations were performed at the Molecular Structure Corporation, College Station, Texas 77840. The following programs were used: DATARED by Frenz for data reduction; MULTAN, a direct methods program based on a version by Main, Woolfson, and Germain. FOURIER by Robinson and Dellaca and based on Zalkin's FORDAP; NUCLS, a full-matrix least-squares program by Ibers and Doedens based on Busing and Levy's ORFLS program; a modified version of SADIAN by Bauer for calculating atomic distances and angles; FAME, based on a version by Dewar with modifications by Goldberg; ORTEP by Johnson for illustrations; the function and error program ORFEE by Busing, Martin, and Levy as modified by Brown, Johnson, and Thiessen; LIST by Snyder for listing data.

(13) D. T. Cromer and D. Liberman, *J. Chem. Phys.*, **53**, 1819 (1971).

(14) D. T. Cromer and J. T. Waber, "International Tables for X-Ray Crystallography", Vol. IV, Kynoch Press, Birmingham, England, 1974, Table 2.3.1.

(15) See paragraph at end of paper concerning supplementary material.

(16) Calculations and refinements for this structure were done on an IBM 360/65 system. Programs used were as above including PERFACT, a program by Frenz for analyzing structure factors and weighting schemes.

(17) M. R. Churchill, *Inorg. Chem.*, **6**, 190 (1967).

(18) In making this comparison, it must be noted that the solvents used for compounds **3** and **4** were not the same and thus the positions of the weak signals of a given isomer as a contaminant in one spectrum are not identical with the positions observed in its "own" spectrum. The solvents (percentages by volume) were as follows: Figure 6, from −85 to 13 °C: 25% CD_2Cl_2, 70% 2-methyltetrahydrofuran, 5% Me_4Si. Figure 7, from −99 to 25 °C; 45% CD_2Cl_2, 50% CCL_3CH_3, 5% Me_4Si. Figure 7, from 27 to 122 °C: 20% C_6D_6, 75% toluene, 5% Me_4Si.

(19) J. Takats and L. Kruczynski, *J. Am. Chem. Soc.*, **96**, 932 (1974).

(20) J. Y. Lallemand, P. Laszlo, C. Muzette, and A. Stockis, *J. Organomet. Chem.*, **91**, 71 (1975).

(21) S. Aime, L. Milone, and E. Sappa, *J. Chem. Soc., Dalton Trans.*, 838 (1976).

(22) F. A. Cotton, D. L. Hunter, and P. Lahuerta, *Inorg. Chem.*, **14**, 511 (1975).

(23) R. D. Adams, F. A. Cotton, W. R. Cullen, D. L. Hunter, and L. Mihichuk, *Inorg. Chem.*, **14**, 1395 (1975).

(24) F. A. Cotton and D. L. Hunter, *J. Am. Chem. Soc.*, **97**, 5739 (1975).

(25) F. A. Cotton, D. L. Hunter, and J. M. Troup, *Inorg. Chem.*, **15**, 63 (1976).

(26) F. A. Cotton and D. L. Hunter, *J. Am. Chem. Soc.*, **98**, 1413 (1976).

A Synthetic Tetranuclear Iron–Sulfur Complex with Ionized Side Chains: The Crystal Structure of $(Fe_4S_4(S(CH_2)_2COO)_4)^{6-}\cdot(Na_5\cdot N(C_4H_9)_4)^{6+}\cdot 5C_5H_9NO$

H. L. Carrell,* [1] Jenny P. Glusker,[1] Robert Job,[2] and Thomas C. Bruice[2]

Contribution from the Institute for Cancer Research, Fox Chase Cancer Center, Philadelphia, Pennsylvania 19111, and the Department of Chemistry, The University of California at Santa Barbara, Santa Barbara, California 93106.

Received July 6, 1976

Abstract: The structure of a synthetic tetranuclear iron–sulfur complex, a model for the active site of ferredoxins, has been determined by x-ray crystallographic techniques. The contents of the asymmetric unit of the crystal consist of one hexanegative anion $(Fe_4S_4(S(CH_2)_2COO)_4)^{6-}$, and six cations (one $N(C_4H_9)_4^+$ and five Na^+). There are also five molecules of *N*-methylpyrrolidone (C_5H_9NO) of crystallization. The unit cell dimensions are $a = 21.088\ (7)$ Å, $b = 31.178\ (10)$ Å, $c = 11.703\ (4)$ Å, $\beta = 92.63\ (2)^\circ$ and the space group is $P2_1/a$. The structure was refined for 17 005 independent data of which 8284 were greater than $2.5\sigma(I)$. The final R value was 0.066 for observed data. The method of preparation is described. This compound is unique among model compounds prepared so far because of its solubility in water. The half-wave potential of the compound is −0.58 V (vs. standard hydrogen electrode), a value similar to the reduction potential of a natural ferredoxin (−0.53 to −0.58 V). The iron–sulfur cluster is a distorted cube, squashed by 0.04 Å in one direction. The side chains of the cluster extend in a direction parallel to the b axis toward a column of sodium cations which extends in the c direction throughout the crystal. The oxygen atoms of *N*-methylpyrrolidone molecules take part in the coordination around sodium atoms. Clusters in adjacent unit cells pack 11.7 Å apart (c axis) with a tetrabutylammonium ion between two such clusters. There appears to be some interaction between the hydrophobic chains of the cation and some of the sulfur atoms of the cluster compound.

Nonheme iron–sulfur proteins are found in many bacterial, plant, and animal cells and act as electron carriers in these systems. Many such proteins contain an Fe_4S_4* cluster,[3] shaped approximately as a distorted cube with iron and sulfur atoms at alternate corners.[4]

Our knowledge of the Fe_4S_4* clusters comes from structural studies of both proteins containing such clusters and from similar studies of model compounds. Proteins which contain these clusters and that have been studied by x-ray crystallographic techniques include the ferredoxin from *P. aerogenes*[5] (two Fe_4S_4* clusters per molecule) and the high-potential iron–sulfur protein (HiPIP) from *Chromatium*[6] (one Fe_4S_4* cluster per molecule). However, in order to obtain high resolution data on bond lengths and angles, some model compounds with the formulas $[Fe_4S_4(SR)_4]^{2-}$ have been prepared by Holm and studied chemically and crystallographically.[7-9] In these model compounds, where R = $-CH_2C_6H_5$[7,8] or $-C_6H_5$[9], the dimensions of the cube-like cluster have been determined.